The 9th European Congress on Computational Methods in Applied Sciences and Engineering
ECCOMAS Congress 2024
3–7 June 2024, Lisboa, Portugal

MATHEMATICAL AND NUMERICAL APPROACH OF ENCAPSULATED PHASE CHANGE MATERIAL IN STRUCTURED THERMOCLINE SYSTEMS

Oriol Sanmartí, Jordi Vera, Santiago Torras and Carlos D. Pérez-Segarra*

Heat and Mass Transfer Technological Center (CTTC), Technical University of Catalonia - BarcelonaTech (UPC), Carrer de Colom 11, 08222 Terrassa (Barcelona), Spain
e-mail: cdavid.perez.segarra@upc.edu

Key words: Unsteady one-dimensional model, Finite volume method, Encapsulated phase change material, Structured thermocline, Thermal energy storage

Summary. An unsteady one-dimensional computational model has been developed to investigate the integration of encapsulated phase change materials in a structured thermal energy storage system. The model has been validated against experimental results available in the literature. The study examines three different phase change materials (NaNO3, KOH, and H380), focusing on how the accumulated energy varies with the thickness of the phase change material layer and the proximity of the melting point to the system's operating temperatures.

1 INTRODUCTION

The intermittent nature of renewable energies may delay their rapid growth. To overcome this challenge, novel energy storage methods or enhancements to existing ones are required. Thermal energy storage has been extensively studied as a potential solution to this issue. These systems can be used in conjunction with concentrated solar power, where molten salt is used as a heat transfer fluid. However, molten salt is the most expensive component of these systems. Therefore, in recent years, alternatives have been studied where only a single tank is needed, and a solid filler and encapsulated phase change material (EPCM) is used to substitute a part of the fluid. A promising alternative that has emerged in recent years is the use of structured solid filler materials made from waste materials such as ceramics or concrete [1].

A promising approach to advance the development of structured thermoclines is to integrate EPCM into this innovative type of system [2]. The objective of this study is to develop a mathematical and numerical model that couples the EPCM in both spheres and tubes with structured thermoclines. The model involves a one-dimensional discretization of the filler material structure, with another one-dimensional discretization of spheres or tubes applied in the EPCM regions. The energy equation is solved using an enthalpy method to account for phase change. Unlike other one-dimensional EPCM models in the literature [3], an innovative aspect of this model lies in its capability to account for volume changes of the phase change material inside the spheres or tubes during the transition from solid to liquid states. This is achieved by integrating the mass equation, leading to changes in the apparent diameter of the EPCM domain while maintaining a constant diameter of the spheres or tubes.

This study is innovative in its aspiration to integrate an existing technology (EPCM) into a novel thermal energy storage system (structured thermocline). After the model is validated

against experimental data, it is used to obtain the accumulated energy for three different materials (NaNO3, KOH, H380) in function of the thickness of the phase change material layer and the proximity of the melting point to the system's operating temperatures.

2 METHODOLOGY

2.1 Case geometry

The thermal energy storage (TES) system under study is a structured type that incorporates encapsulated phase change material in tube format, with an outer diameter of 33.7mm, a thickness of 2mm, and a void fraction between the molten salt and the tubes of 0.47. The geometrical design includes a solid filler material composed of waste ceramic products. The ceramic matrix has perforations through which molten salt flows, facilitating thermal energy storage. The TES system is depicted in Figure 1, showcasing two configurations: one with the EPCM positioned at the bottom and the other with the EPCM at the top. The structure includes a buffer region at the top and a sump region at the bottom, which zones are used to extract or inject the fluid and give some thermal inertia to the system.

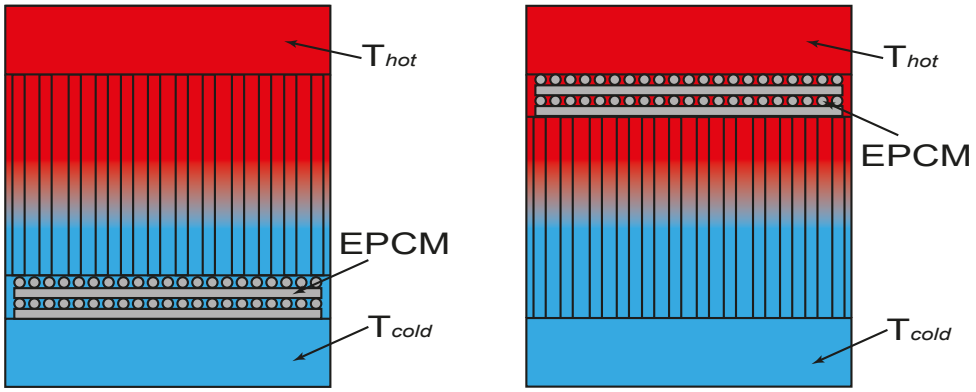

Figure 1: Thermocline structured geometry representation with EPCM positioned at the bottom (left) and top (right). Figure extracted from [4].

Regarding the two studied cycles, during the charging process, molten salt flows from the top to the bottom of the tank until the temperature at the bottom reaches a predetermined cutoff temperature. Conversely, the flow direction reverses during the discharging process, and molten salt is discharged from the bottom to the top until the top temperature achieves the cutoff temperature. Table 1 shows the main geometrical and operational parameters used in the simulations.

Table 1: Main geometrical and operational parameters considered in this study.

Parameter	Acronym	Value
Tank diameter	D_{tank}	45 m
Height of the sump region	h_{bot}	1 m
Height of the tank bed	h_{bed}	11.5 m
Height of the buffer region (at T_{cold})	h_{top}	0.5 m
Channel diameter	d	0.01 m
Distance between channels	L_{tp}	0.02 m
Channels arrangement	Arr.	30°C
Hot temperature	T_{hot}	385°C
Cold temperature	T_{cold}	290°C
Cutoff temperature difference	ΔT_{co}	15°C
Overall tank mass flow charge	$\dot{m}^{\text{c}}_{\text{all}}$	1635 kg/s
Overall tank mass flow discharge	$\dot{m}^{\text{d}}_{\text{all}}$	837 kg/s

2.2 Governing equations

The molten salt and filler material are modelled using a one-dimensional discretization along the axial direction, divided into N control volumes (CVs). The equations presented by Schumann in 1929 [5] are solved for a porous solid in contact with a fluid. These equations are enhanced by modifying the wetted area to consider the convection with all the tubes instead of the traditional solid particles. The energy conservation equations for molten salt and solid filler material are given in Equations (1) and (2). The encapsulated phase change material is modelled with a radial discretization for each of the N control volumes, using M CVs in the radial direction. The energy conservation equation includes the latent heat by relating enthalpy and temperature, as shown in Equation (3). Convective terms are applied as boundary conditions. Special energy balances are applied for the buffer and sump regions. The governing equations are as follows:

$$\epsilon \rho_f c_{p,f} \left(\frac{\partial T_f}{\partial t} + v_{z,f} \frac{\partial T_f}{\partial z} \right) = \alpha (T_s - T_f) a_w + \frac{\partial}{\partial z} \left(\lambda_f \frac{\partial T_f}{\partial z} \right) - \dot{q}_{f,lost} \tag{1}$$

$$(1-\epsilon) \rho_s c_{p,s} \left(\frac{\partial T_s}{\partial t} \right) = \alpha (T_f - T_s) a_w + \frac{\partial}{\partial z} \left(\lambda_s \frac{\partial T_s}{\partial z} \right) - \dot{q}_{s,lost} \tag{2}$$

$$\rho_{pcm} \left(\frac{\partial h_{pcm}}{\partial t} \right) = \frac{\partial}{\partial r} \left(\lambda_{pcm} \frac{\partial T_{pcm}}{\partial r} \right) \tag{3}$$

In these equations, ρ, λ, and c_p are the density, thermal conductivity, and specific heat, respectively, α is the local heat transfer coefficient, and ϵ the void fraction, which is the molten salt volume relative to the total volume. a_w is the wetted area per unit volume, $v_{z,f}$ the velocity of the fluid flow, and $\dot{q}_{lost}$ represents the heat losses per unit volume to the ambient. The subindex f refers to the fluid, and the subindex s refers to the solid. For the case inside the channels in the structured thermocline, the empirical correlation for Nusselt is obtained following Taborek et al.'s correlations [6]. In the case of the EPCM, a correlation for tubes in cross-flow is used, following the work of Zukauskas [7].

2.3 Thermophysical properties

The properties of the molten salt, specifically Solar Salt, are taken from Zavoico et al. [8]. The solid filler material has a density of 2785 kg/m^3, a thermal conductivity of 0.57 W/mK, and a specific heat capacity of 1148 J/kgK. Finally, Table 2 presents the properties of the PCMs examined in this study.

Table 2: Thermophysical properties of the used PCM.

Property	$NaNO_3$ [9]	KOH [10]	H380 [11]
Density (kg/m^3)	2075	2040	2050
Specific heat (kJ/kgK)	1444	1340	1530
Latent heat (J/kg)	1.75E5	1.34E5	2.25E5
Thermal conductivity (W/mK)	0.5	0.5	0.56
Melting Point (°C)	306	380	382

3 CODE VERIFICATION AND VALIDATION

For the verification of the code and validation of the mathematical formulation, an experimental setup is simulated to compare the computational results with the ones obtained in the experiments. The experimental setup, presented by Keilany et al. [12], comprises a thermal energy storage system with several key parameters. The storage tank has a diameter of 1.2 meters and a filler height of 2.53 meters. The system starts at an initial temperature of 312°C, the maximum temperature achieved during the experiment, indicating the upper limit of the temperature range. The minimum temperature observed in the system is 226°C, marking the lower limit during the cycle. The experiment simulates a discharge cycle, extracting thermal energy from the storage material. The heat transfer fluid used in the system is Jarytherm Oil, with a mass flow rate of 0.555 kg/s. The EPCM used is sodium nitrate (NaNO3), configured as a tube to provide a specific surface area for heat exchange. The filler material in the tank is Alumina (Packed Bed distribution), which provides structural support and thermal conductivity.

Figure 2 compares the experimental results and the computational results derived from the model proposed in this study. The temperature profiles shift from left to right, starting from a uniform temperature of 312 ºC. The temperature profiles exhibit a very similar pattern, and a change in the slope of the profile can be observed on the right side of the plot. This change corresponds to the location of the EPCM changing phase. The results obtained from this comparison are satisfactory for validating the mathematical formulation. Additionally, a numerical study was conducted to determine the appropriate number of nodes and time steps, verifying that the simulation results are independent of these parameters. The structured layer of the thermocline has been validated against the computational results of Vera et al. [13, 14]. Although the model can consider heat losses to the exterior, such losses have been neglected in this study.

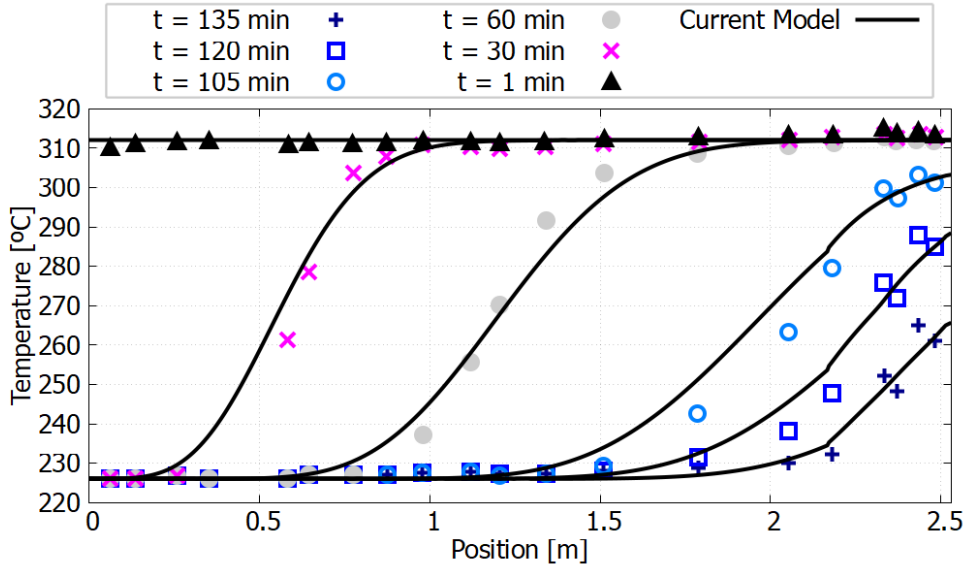

Figure 2: Comparison with the experimental results of Keilany et al. [12] for temperature profiles over time.

4 RESULTS

The previously presented structure is simulated, incorporating the three alternatives for the EPCM: NaNO3, KOH, and H380. The EPCM is positioned at the lower part for the NaNO3 case and the upper part for the H380 and KOH cases. Results are obtained for the accumulated energy in each of the three cases, considering the thickness of the phase change material layer and the proximity of the melting temperature to the system's operating temperature. All the presented results are obtained under cyclic periodic conditions.

Figure 3 shows the accumulated energy relative to the EPCM thickness, which is the percentage of EPCM relative to the total height of the filler material. In all cases, optimal results are achieved when utilizing a small EPCM height relative to the total height of the filler material bed. NaNO3 exhibits poor performance and, in some cases, even negative performance. This could be attributed to its melting temperature of 306 °C. With a cut-off temperature difference of 15 °C and a cold temperature of 290 °C, it falls outside the melting/solidification range of the EPCM.

It can be observed that despite the less favourable physical properties of energy density and latent heat for KOH, it exhibits superior performance across all heights and lower cutoff temperature differences. This observation may be attributed to temperature differences of the hot/cold temperature, the EPCM's melting temperature, and the cutoff temperature difference. H380*, which is a fictional EPCM with 380 °C as a melting temperature, is simulated, and it can be seen that it exhibits superior performance for all thicknesses due to its better thermophysical properties and the same melting temperature as KOH.

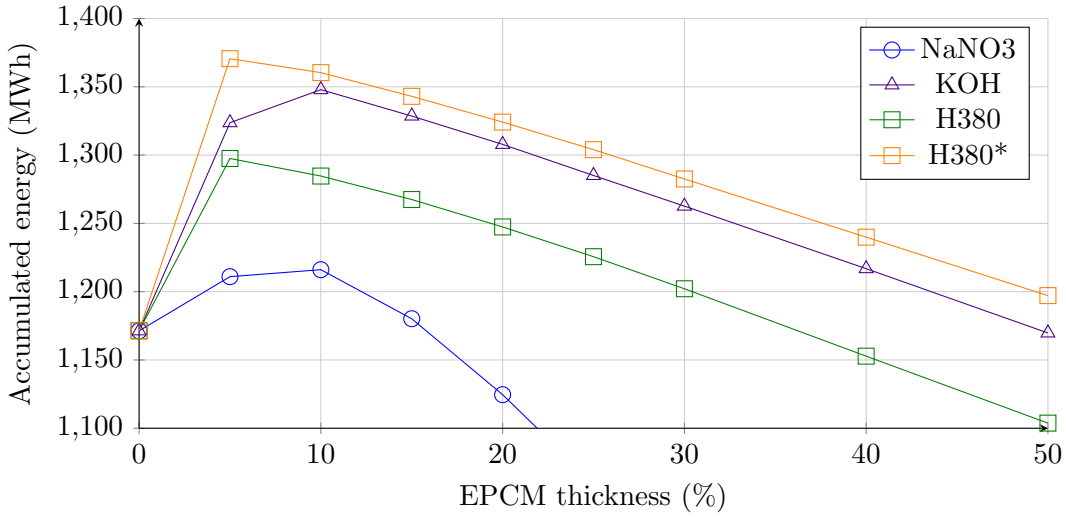

Figure 3: Accumulated energy as a function of thickness percentage of EPCM for three materials as EPCM for a cutoff temperature difference of 15°C.

In Figure 4, the accumulated energy is evaluated for a fictional EPCM where its melting temperature is considered as the distance between the hot region for the top EPCMs and the cold region for the bottom EPCMs. Given a cut-off temperature of 15 °C, the EPCM's effectiveness diminishes if the temperature difference exceeds this threshold. The top EPCMs (H380 and KOH) perform well within the 10-15 °C range, whereas the bottom EPCM (NaNO3) begins to decline in effectiveness when the temperature difference surpasses 10 °C.

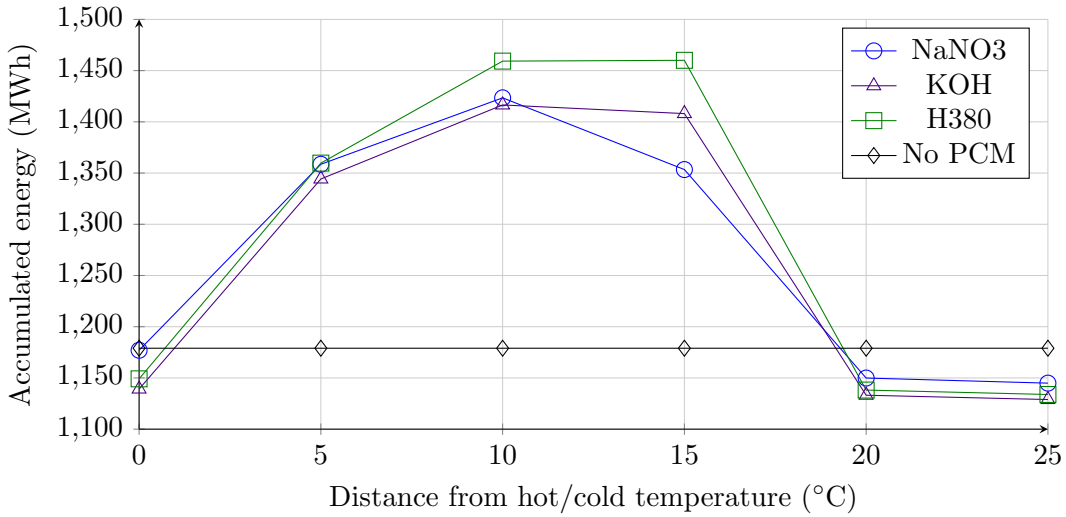

Figure 4: Accumulated energy as a function of the distance of the melting temperature from the hot/cold temperature for three materials as EPCM and without EPCM for a cutoff temperature difference of 15°C and a EPCM thickness of 10 %.

5 CONCLUSIONS

The integration of encapsulated phase change material in a structured thermal energy storage system is studied. The fluid and filler material are discretised using an unsteady one-dimensional approach, while the EPCM is discretised one-dimensionally in the radial direction. The model is well-verified and validated using experimental results from other authors. Optimal results are achieved when the EPCM constitutes a small part of the height relative to the filler material bed and a distance between the melting point and the hot/cold regions of 10-15 °C.

Despite KOH having thermally unfavourable properties, it exhibits superior performance. NaNO3 demonstrates poor performance at low cutoff temperature differences due to its high melting temperature (306 °C) with respect to the cold temperature (290°C), preventing melting at low cutoff temperatures. H380 possesses favourable thermal properties, but its relatively high melting temperature (382 °C), close to the hot temperature (385 °C), limits its latent heat energy utilisation. H380* has a better behaviour than KOH, confirming the importance of the distance of the melting temperature from the hot temperature. The top EPCMs (H380 and KOH) perform well within the 10-15 ºC range (close to the 15 °C cutoff temperature), whereas the bottom EPCM (NaNO3) begins to decline in effectiveness when the temperature difference surpasses 10 °C.

In future work, a more detailed study will be conducted on the EPCM thickness and the distance of the melting temperature of different materials from the hot/cold temperatures for various cut-off temperatures and different EPCM thicknesses. This study will be valuable for determining the optimal material for a specific structured TES, as well as identifying the ideal operational parameters to maximize the potential of the EPCM.

6 ACKNOWLEDGEMENTS

This work is carried out in the framework of the Newcline project. It is supported under the umbrella of CSP-ERA.NET 1st Cofund Joint Call and by the following National Agencies: AEI (Spain), CDTI (Spain), Jülich (Germany), SFOE (Switzerland). CSP-ERA.NET is supported by the European Commission within the EU Framework Programme for Research and Innovation Horizon 2020 (Cofund ERA-NET Action, Nº 838311). The first author acknowledges the financial support from the "Departament de Recerca i Universitats de la Generalitat de Catalunya" and the "Fons Social Europeu" with the predoctoral grant JOAN ORÓ FI AGAUR (2023 FI 00192).

REFERENCES

[1] L. Boquera, J.R. Castro, A.L. Pisello, L.F. Cabeza, "Research progress and trends on the use of concrete as thermal energy storage material through bibliometric analysis," *J. Energy Storage*, vol. 38, p. 102562, 2021. DOI: 10.1016/j.est.2021.102562.

[2] O. Sanmartí, J. Vera, S. Torras, C.D. Pérez-Segarra, "Parametric study for a structured thermal energy storage system for concentrated solar power plants," *Energy*, vol. 305, p. 132271, 2024. DOI: 10.1016/j.energy.2024.132271.

[3] P.A. Galione, C.D. Pérez-Segarra, L. Rodríguez, A. Oliva, J. Rigola, "Multi-layered solid-PCM thermocline thermal storage concept for CSP plants. Numerical analysis and perspectives," *Appl. Energy*, vol. 142, pp. 337–351, 2015. DOI: 10.1016/j.apenergy.2014.12.084.

[4] O. Sanmartí, J. Vera, S. Torras, C.D. Pérez-Segarra, "Numerical investigation of phase change material integration in structured thermocline systems for concentrated solar power," *Journal of Physics: Conference Series*, vol. 2766, no. 1, p. 012216, 2024. DOI: 10.1088/1742-6596/2766/1/012216.

[5] T.E.W. Schumann, "Heat transfer: A liquid flowing through a porous prism," *J. Frankl. Inst.*, vol. 208, pp. 405–416, 1929. DOI: 10.1016/S0016-0032(29)91186-8.

[6] J. Taborek, "Double-Pipe and Multitube Heat Exchangers with Plain and Longitudinal Finned Tubes," *Heat Transfer Engineering*, vol. 18, pp. 34–45, 1997. DOI: 10.1080/01457639708939894.

[7] A. Žukauskas, "Heat Transfer from Tubes in Crossflow," in *Advances in Heat Transfer*, vol. 8, J.P. Hartnett and T.F. Irvine, Eds. Elsevier, pp. 93–160, 1972. DOI: 10.1016/S0065-2717(08)70118-7.

[8] A.B. Zavoico, *Solar Power Tower Design Basis Document, Revision 0*, Sandia National Lab. (SNL-NM), Albuquerque, NM (United States); Sandia National Lab. (SNL-CA), Livermore, CA (United States), 2001. DOI: 10.2172/786629.

[9] T. Bauer, D. Laing, R. Tamme, "Characterization of Sodium Nitrate as Phase Change Material," *Int. J. Thermophys.*, vol. 33, pp. 91–104, 2011. DOI: 10.1007/s10765-011-1113-9.

[10] M.A. Geyer, "Thermal Storage for Solar Power Plants," in *Solar Power Plants: Fundamentals, Technology, Systems, Economics*, C.-J. Winter, R.L. Sizmann, L.L. Vant-Hull, Eds. Berlin, Heidelberg: Springer, pp. 199–214, 1991. ISBN: 978-3-642-61245-9.

[11] A. Crespo, C. Barreneche, M. Ibarra, W. Platzer, "Latent thermal energy storage for solar process heat applications at medium-high temperatures – A review," *Sol. Energy*, vol. 192, pp. 3–34, 2019. DOI: 10.1016/J.SOLENER.2018.06.101.

[12] M.A. Keilany, S. Vannerem, M. Milhé, Q. Falcoz, J.-J. Bézian, G. Flamant, "Experimental and numerical study of combining encapsulated phase change material to sensible heat storage material in one-tank pilot scale thermal energy storage," *J. Energy Storage*, vol. 51, p. 104504, 2022. DOI: 10.1016/j.est.2022.104504.

[13] J. Vera Fernandez, G. Colomer, O. Sanmartí, C. Perez, "Modelization of a molten salt thermal energy storage for concentrated solar power," in *8th European Congress on Computational Methods in Applied Sciences and Engineering*, 2022. DOI: 10.23967/eccomas.2022.182.

[14] J. Vera Fernandez, O. Sanmartí, S. Torras, C.D. Perez Segarra, "Parametric Study of Structured Thermocline Storage Systems," in *EuroSun 2022 - ISES and IEA SHC International Conference on Solar Energy for Buildings and Industry*, 2022. DOI: 10.18086/eurosun.2022.13.22.